



Published in final edited form as:

J Immunol. 2011 December 15; 187(12): 6301–6309. doi:10.4049/jimmunol.1100891.

Granzyme B Regulates Antiviral CD8⁺ T cell Responses¹

Suzan M. Salti^{*}, Erin M. Hammelev^{*}, Jenny L. Grewal^{*}, Sreelatha T. Reddy^{*}, Sara Zemple^{*}, William J. Grossman[†], Mitchell H. Grayson^{*}, and James W. Verbsky^{*}

^{*}Departments of Pediatrics and Microbiology and Molecular Genetics, Medical College of Wisconsin, Milwaukee, WI 53226

[†]Biothera, Eagan, MN 55127

Abstract

Cytotoxic T lymphocytes and natural killer cells utilize the perforin/granzyme cytotoxic pathway to kill virally-infected cells and tumors. Human regulatory T cells also express functional granzymes and perforin and can induce autologous target cell death *in vitro*. Perforin-deficient mice die from excessive immune responses after viral challenges, implicating a potential role for this pathway in immune regulation. To further investigate the role of granzyme B in immune regulation in response to viral infections, we characterized the immune response in wild-type, granzyme B deficient, and perforin deficient mice infected with Sendai virus. Interestingly, granzyme B deficient mice, and to a lesser extent perforin deficient mice, exhibited a significant increase in the number of Ag-specific CD8⁺ T cells in the lungs and draining lymph nodes of virally infected animals. This increase was not the result of failure in viral clearance since viral titers in granzyme B-deficient mice were similar to wild-type mice and significantly less than perforin-deficient mice. Regulatory T cells from WT mice expressed high levels of granzyme B in response to infection, and depletion of regulatory T cells from these mice resulted in an increase in the number of Ag-specific CD8⁺ T cells, similar to that observed in granzyme B-deficient mice. Furthermore, granzyme B-deficient regulatory T cells displayed defective suppression of CD8⁺ T cell proliferation *in vitro*. Taken together these results suggest a role for granzyme B in the regulatory T cell compartment in immune regulation to viral infections.

Introduction

Cytotoxic CD8⁺ T cells and NK cells utilize granzyme (Gzm) and perforin (Prf) molecules packaged in cytotoxic granules to kill virally-infected cells and tumors. Gzms are known to activate target cell apoptosis through caspase-dependent and independent pathways¹, while Prf is implicated in the delivery of these cytotoxic molecules into target cells². Among the Gzm family, GzmB, which cleaves target proteins after aspartate residues, has the strongest proapoptotic function² resulting in DNA fragmentation and rapid loss of membrane integrity. While perforin deficient (*Prfl*^{-/-}) mice are susceptible to a variety of viruses and tumor models, GzmA (*Gzma*^{-/-}) or GzmB-deficient (*Gzmb*^{-/-}) mice show variable resistance to viral and tumor challenges³⁻⁷. This can be explained by the redundancy of granzymes, while there is no redundant molecule for perforin. When mice are deficient in both GzmB and GzmA they exhibit greater susceptibility to certain pathogens compared to *Gzma*^{-/-} or *Gzmb*^{-/-} mice⁸⁻⁹.

Address correspondence and reprint requests to Dr. James W. Verbsky, Department of Pediatrics, 8701 Watertown Plank Road, Medical College of Wisconsin, Milwaukee, WI 53226. jverbsky@mcw.edu.

Disclosures

The authors have no financial conflict of interest.

While the role of Prf and Gzms in viral clearance is well-defined, recent evidence suggests a paradoxical role for this pathway in immune regulation, as demonstrated by the human disease Hemophagocytic Lymphohistiocytosis (HLH). Patients with HLH exhibit uncontrolled immune responses after viral infections evidenced by elevated levels of proinflammatory cytokines, subsequent activation of macrophages, phagocytosis of hematopoietic cells, and tissue damage^{10–12}. All genetic mutations underlying primary HLH are in proteins that are critical for either the functional degranulation of cytotoxic granules (e.g. SAP, Munc13-4, Lyst, Rab27A, Syntaxin 11), or the delivery of their cytotoxic contents into target cells as is the case in Prf deficiency^{10;12}. *Prfl*^{-/-} mice infected with lymphocytic choriomeningitis virus (LCMV) or murine cytomegalovirus (MCMV) develop a HLH-like syndrome due to uncontrolled expansion of Ag-specific CD8⁺ T cells, and excessive production of the proinflammatory cytokines IFN- γ and TNF- α ^{9;13}. While persistence of Ags due to failure in viral clearance likely contributes to the exaggerated immune response, the possibility remains that Prf and other components of the cytotoxic granule pathway may be involved in regulating CD8⁺ T cell responses. This possibility is further supported by recent evidence that GzmB and Prf can be used by T regulatory (T_{reg}) cells to regulate immune responses.

T_{reg} cells are a subset of CD4⁺ T cells that have been shown to control the immune response to auto-, allo-, pathogen-derived, and tumor Ags^{14–17}. They account for 5–10% of CD4⁺ T cells in the periphery, constitutively express CD25^{18–20}, and utilize a variety of mechanisms to suppress immune responses, including cytotoxicity through the Prf/Gzm pathway^{21–23}. Two recent reports have demonstrated that murine CD4⁺CD25⁺ T_{reg} cells upregulate GzmB in response to TCR activation, and can suppress proliferation of CD4⁺CD25⁻ T cells and LPS-activated B cells in a GzmB-dependent manner^{24–25}. Furthermore, CD4⁺CD25⁻ T cells that overexpress the physiologic GzmB inhibitor serine protease inhibitor 6 (Spi6) are resistant to T_{reg} cell suppression^{26–29}. Additionally, *in vitro* activated human T_{reg} cells have been shown to differentially upregulate Gzms, and display Prf-dependent cytotoxicity against a variety of autologous target cells including mature and immature dendritic cells, CD14⁺ monocytes, and activated CD8⁺ and CD4⁺ T cells²¹.

These studies implicate the Gzm/Prf pathway in immune regulation, possibly through the T_{reg} cell compartment. Since little is known about the role of GzmB in immune regulation following viral infections, we set out to characterize the immune response of wild-type (WT) mice, *Gzmb*^{-/-} mice, and *Prfl*^{-/-} mice to Sendai Virus (SeV). SeV is a mouse parainfluenza type I virus that causes severe descending bronchiolitis in rodents^{30–32}. Resolution of primary SeV infection is strictly CD8⁺ T cell-dependent^{33;34}, and infection of WT C57BL/6 mice with SeV is known to elicit a potent CD8⁺ T cell response that is almost exclusively directed at a single K^b-restricted nucleoprotein epitope (NP 324–332)^{35–38}. This allows the use of a class I tetramer loaded with NP 324–332 to characterize Ag-specific CD8⁺ T cell responses to SeV infection. Using this model, we found that SeV-infected *Gzmb*^{-/-} mice displayed great weight loss compared with WT mice that correlated with an increase in the number of Ag-specific CD8⁺ T cells despite efficiently clearing the virus. Furthermore, this phenotype was T_{reg} cell-dependent suggesting that GzmB is important for the ability of T_{reg} cells to regulate Ag-specific CD8⁺ T cell responses.

Materials and Methods

Mice

WT C57BL/6J mice were obtained from the Jackson Laboratory (Bar Harbor, ME). *Prfl*^{-/-} mice containing the “Kagi” mutation³ and *Gzmb*^{-/-} mice³⁹ were a kind gift from Timothy J. Ley, and were backcrossed for eleven generations onto the C57BL/6J strain. The *Gzmb*^{-/-} mice were the *Gzmb*^{-/-}-Cre mice, and thus only *Gzmb*^{-/-} was deficient. Foxp3^{EGFP} mice

contain a bicistronic *FoxP3* locus that express GFP under the control of the endogenous/enhancer elements of *FoxP3*, a transcription factor required for the development and function of T_{reg} cells¹⁶. Foxp3^{EGFP} mice were a kind gift from Talal A. Chatila (University of California-Los Angeles) and were crossed to *Gzmb*^{-/-} mice and *Prfl*^{-/-} mice. All mice were bred and housed under specific pathogen-free conditions, and all experiments were conducted in accordance with the guidelines of the institutional Animal Research Committee at the Medical College of Wisconsin.

Viral infection

Male mice of 6–12 weeks of age were anesthetized with ketamine and xylazine, and inoculated intranasally with 6×10^4 PFU of SeV (Fushimi strain, ATCC) in 30 μ l of PBS. This dose was used since preliminary experiments with 2×10^5 PFU resulted in excessive mortality in *Prfl*^{-/-} mice. Individual mice were weighed before and every day after infection. Percentage of baseline weight loss was calculated using the following formula: [weight/weight at day 0] * 100%.

Lung SeV titer

Lungs were harvested from mice sacrificed at day 10, flash frozen in liquid nitrogen, then homogenized in TRIzol reagent (Invitrogen Life Technologies, Carlsbad, CA) to extract RNA. cDNA was synthesized from 4 μ g of RNA using QuantiTect Reverse Transcription cDNA synthesis kit (Applied Biosystems, Foster City, CA), and SeV *nucleocapsid* gene expression was measured by real-time quantitative PCR using Taqman PCR Master Mix (Applied Biosystems). The primers and probes were developed in Dr. Michael Holtzman's laboratory at Washington University in St. Louis⁴⁰. The *gapdh* house keeping gene was detected in the cDNA samples using *Gapdh* primers and probe (Applied Biosystems). Construct standard curves were used for quantification as previously described³².

Antibodies

Fluorochrome-labeled antibodies were utilized according to the manufacturers' recommendations as follows: Pacific Blue anti-CD4 (RM4-5), Pacific Orange anti-CD8a (5H10), and R-PE anti-Granzyme B (GB12) were from Invitrogen Life Technologies (Carlsbad, CA); PE-Cy7 anti-CD11c (HL3), PE-Cy7 anti-IFN- γ (XMG1.2), PE-Cy7 anti-CD25 (PC61) were from BD PharMingen (San Diego, CA); PE-Cy5.5 anti-CD19 (eBio1D3), PE anti-CD62L (MEL-14), PE-Cy7 anti-NK1.1 (PK136) were from eBioscience (San Diego, CA); Alexa 700 anti-CD44 (IM7) was from Biolegend (San Diego, CA); functional grade Rat IgG1 (HRPN) was from Bio X Cell (West Lebanon, NH). PC61 (anti-CD25 mAb) and 2C11 (anti-CD3 mAb) hybridomas were purchased from the American Tissue Culture Collection (Manassas, VA), and Abs were generated and purified from tissue-cultured supernatants.

Flow cytometry

Lungs and draining lymph nodes were harvested at indicated time points. Lungs were minced, and digested at 37°C for 60 min in media containing DMEM supplemented with 10% FBS, 1% glutamine, 1% non essential amino acids, 1% sodium pyruvate, 1% penicillin/streptomycin, 10 mM HEPES (Invitrogen Life Technologies), 250 U/ml collagenase I, 50 U/ml DNase I (Worthington Biomedical, Lakewood, NJ), and 0.01% hyaluronidase (Sigma-Aldrich, St. Louis, MO). During the last 15 min of incubation time, EDTA (Fisher Scientific, Hanover Park, IL) was added to the medium to a final concentration of 2 mM. After digestion, single-cell suspensions were obtained by passing the cell mixture through a 40 μ m cell strainer, then erythrocytes were removed by hypotonic lysis. Recovered cells were then enumerated for total cell count and stained for cell surface markers. Ag-specific

CD8⁺ T cells were detected using a MHC-peptide tetramer specific for SeV nucleoprotein NP324–332 provided by the National Institute of Allergy and Infectious Disease Tetramer Core Facility (Bethesda, MD). Intracellular staining for GzmB was conducted using BD Cytotfix/Cytoperm and BD Perm/Wash buffers (BD Biosciences, San Jose, CA) according to the manufacturer's recommendations. To detect intracellular IFN- γ , cells isolated from infected lungs were incubated with 50 ng/ml PMA (Sigma-Aldrich), 500 ng/ml ionomycin (Sigma-Aldrich), and 10 mg/ml brefeldin A (Sigma-Aldrich) for 4 h at 37°C and stained as described earlier. Samples were analyzed on an LSRII (BD Biosciences) and FlowJo software (Tree Star, Ashland, OR). A minimum of 1×10^6 live cell events were collected per sample.

T_{reg} cell depletion with a blocking anti-CD25 mAb

Mice were depleted of T_{reg} cells by intraperitoneal injection of 300 μ g of anti-CD25 (PC61) mAb (or rat IgG1 control Ab) at day -3 and day -1 of SeV infection. This mAb is known to antagonize T_{reg} cell function and results in a reduction in the number of CD4⁺ CD25⁺ T_{reg} cells in the peripheral lymphoid tissues^{41–42}.

CD8⁺ T Suppression assays

CD4⁺ T cells were enriched from whole splenocytes by magnetic cell sorting using CD4 Microbeads and MACS columns (Miltenyl Biotec Inc., Auburn, CA), and CD4⁺EGFP⁺ T_{reg} cells were further purified by cell sorting using a FACS ARIA (BD Biosciences). CD8⁺ T cells were isolated by cell sorting. Cell purity was more than 97% for all experiments. T-cell depleted splenocytes (TdS) were irradiated with 5000 rad. Purified cell populations were suspended in DMEM supplemented with 10% (v/v) fetal bovine serum (FBS), 1% glutamine, 1% non essential amino acids, 1% sodium pyruvate, 1% penicillin/streptomycin, and 10 mM HEPES. 5×10^4 CD8⁺ T cells were added to each well in flat-bottom microtiter plates, and were cultured in the presence of 1.5×10^5 APCs and 5 μ g/ml of anti-CD3 Ab, with either WT or *Gzmb*^{-/-} T_{reg} cells to achieve the indicated suppressor cells to target cells ratios (S:T). Cultures were incubated for 72 h at 37°C with 5% CO₂, pulsed with 0.2 μ Ci/well [³H] thymidine for an additional 18 h, harvested onto fiber filtermats using a Micro96 harvester (Skatron), and counted.

Statistical analysis

Student's unpaired *t* test (for comparison of two groups), or one-way or two-way ANOVA (for comparison of multiple groups) followed by Tukey's multiple comparison test were performed using Prism software (Graph Pad, San Diego, CA) to determine significance. Unless otherwise stated, all data are presented as mean \pm SEM.

Results

SeV infection and viral clearance in *Gzmb*^{-/-} mice and *Prf1*^{-/-} mice

To examine the role of GzmB in SeV infection, we infected WT mice, *Gzmb*^{-/-} mice, and *Prf1*^{-/-} mice with SeV. SeV infection in mice induces an acute inflammatory response accompanied by significant weight loss³². *Gzmb*^{-/-} mice infected with SeV lost more weight and took longer to recover than WT mice (Fig. 1A). In comparison, *Prf1*^{-/-} mice exhibited the greatest weight loss. H&E-stained lung sections from all mice showed peribronchial lymphocyte-rich inflammatory infiltrates, as well as dispersed areas of alveolitis and capillary congestion. Sheets of apoptotic bronchiolar epithelium desquamating into the lumen indicating more severe pathology were observed in *Prf1*^{-/-} mice and, to a lesser extent, in *Gzmb*^{-/-} mice, but not WT mice (data not shown).

We next determined if the absence of GzmB affects viral clearance by measuring viral titers from total lung homogenate by quantitative real-time RT-PCR at day 10 of infection. The results of this assay have been shown to correlate with viral plaque assay and expression of SeV proteins as detected by western blotting³². *Prf1*^{-/-} mice displayed a significant increase in viral titers compared with WT mice, consistent with the well-established role of Prf in viral clearance. *Gzmb*^{-/-} mice, on the other hand, exhibited similar viral titers to WT mice at both 7 and 10 days after infection, indicating that GzmB is not essential for clearance of SeV (Fig. 1B).

Expansion of CD8⁺ T cell compartment in the lungs of *Gzmb*^{-/-} mice and *Prf1*^{-/-} mice in response to SeV infection

While *Gzmb*^{-/-} mice did not appear to have a defect in SeV clearance, they clearly exhibited a less favorable outcome to infection, likely due to immune-mediated pathology. To address whether GzmB has a role in regulating anti-viral immune responses, we characterized the magnitude of Ag-specific CD8⁺ T cell responses in the lungs and draining lymph nodes of these mice. Upon infection with SeV, CD8⁺ T cells in the lungs of *Gzmb*^{-/-} and *Prf1*^{-/-} mice underwent a significant expansion compared to WT mice, with a concomitant decrease in the percentages of CD4⁺ T cells (Fig. 2A, left panel). This was confirmed by determining absolute numbers of CD4⁺ and CD8⁺ T cells in the lungs following infection (Fig. 2A, right panel). Furthermore, *Gzmb*^{-/-} mice, and to a lesser extent *Prf1*^{-/-} mice, exhibited a significant increase in the percentages of Ag-specific CD8⁺ T cells at day 10 of infection (Fig. 2B–C). Similar results were obtained when absolute cell counts were analyzed (data not shown). There was no statistically significant differences in the percentages or absolute numbers of CD19⁺ cells (B-cells), CD11c⁺ cells (dendritic cells), or NK1.1⁺ cells (NK cells) (data not shown).

We also examined the Ag-specific CD8⁺ T cell response in the para-tracheal draining lymph nodes of infected mice. In contrast to the lungs, there was no relative expansion of CD8⁺ cells in the draining lymph nodes of *Gzmb*^{-/-} mice or *Prf1*^{-/-} mice and total lymphocyte numbers in the draining lymph nodes of these mice were comparable to those of WT mice (data not shown). There was, however, a definite increase in the percentages and absolute numbers of Ag-specific CD8⁺ T cells in the draining lymph nodes of *Gzmb*^{-/-} mice but not *Prf1*^{-/-} mice (Fig. 2B–C and data not shown). The percentages and absolute numbers of other cell types (CD19⁺ cells, CD11c⁺ cells, and NK1.1⁺ cells) were comparable to those of WT mice (data not shown).

In addition to their cytotoxic function, CD8⁺ T cells are efficient producers of antiviral cytokines such as IFN- γ . Therefore, we investigated the ability of Ag-specific CD8⁺ T cells from the lungs of WT mice, *Gzmb*^{-/-} mice, and *Prf1*^{-/-} mice to produce IFN- γ . Ag-specific CD8⁺ T cells from all mice produced IFN- γ in response to PMA/ionomycin stimulation to a similar magnitude (Fig 3A). However, *Gzmb*^{-/-} mice displayed a relative increase in the percent and number of IFN- γ ⁺ CD8⁺ T cells due to the underlying expansion of Ag-specific CD8⁺ T cells in these mice.

To determine whether GzmB plays a role in regulating the activation state of immune effector cells, we investigated the expression of memory-activation markers CD44, CD62L, and CD25 on CD8⁺ T cells in SeV-infected mice. Not surprisingly, similar to what has been described in WT mice⁴³, almost all Ag-specific CD8⁺ T cells in the lungs of *Gzmb*^{-/-} mice were of the effector memory (CD44^{hi}CD62L^{lo}) phenotype (data not shown). Interestingly, there was a significant increase in the percentage of CD25⁺Ag-specific CD8⁺ T cells in the lungs of *Gzmb*^{-/-} mice compared to WT mice (Fig. 3B). This phenotype was even more pronounced in the draining lymph nodes where up to 60% of Ag-specific CD8⁺ T cells in *Gzmb*^{-/-} mice expressed high levels of CD25 (Fig. 3B). On the other hand, CD25

expression in T_{reg} cells and conventional $CD4^+$ T cells was not significantly affected by the lack of GzmB. Taken together, these data argue that GzmB has a role in regulating the magnitude and activation status of Ag-specific $CD8^+$ T cell responses to SeV.

Expression patterns of GzmB in lymphocytes in the lungs and draining lymph nodes of SeV-infected mice

To further investigate the source of GzmB responsible for regulating Ag-specific $CD8^+$ T cell activation/expansion, we examined the expression pattern of GzmB in the lungs and draining lymph nodes of $Foxp3^{EGFP}$ mice during SeV infection. Not surprisingly, at day 10, GzmB was expressed in the majority of NK cells ($NK1.1^+$ cells), Ag-specific $CD8^+$ T cells, and to a lesser extent, non Ag-specific $CD8^+$ T cells isolated from the lungs of WT mice (Fig. 4A–B) and $Prf1^{-/-}$ mice (data not shown). Interestingly, while only a limited percentage of conventional $CD4^+$ T cells expressed GzmB, a significantly larger percentage of T_{reg} cells in the lungs of infected mice upregulated GzmB (Fig. 4A–B). In the draining lymph nodes, around 55% of Ag-specific $CD8^+$ T cells and 5–10% of T_{reg} cells expressed GzmB, with minimal expression in conventional $CD4^+$ T cells (Fig. 4B). Indeed, when absolute counts were analyzed there were roughly equal numbers of $GzmB^+$ T_{reg} cells and $GzmB^+$ Ag-specific $CD8^+$ T cells in the draining lymph nodes of WT mice (Fig. 4C).

T_{reg} cells are recruited to the lungs of infected mice

We next examined the kinetics of lymphocyte recruitment to the lungs, and GzmB expression by these cells in response to SeV infection. At day 7, we observed a doubling in the absolute numbers of $FoxP3^+$ T_{reg} cells in the lungs of WT mice in both WT mice and $Gzmb^{-/-}$ mice (Fig. 5A), indicating that these molecules probably do not play a significant role in the expansion or contraction of T_{reg} cells. Expression of GzmB in WT T_{reg} cells also peaked at day 7, with a high percentage of T_{reg} cells in the lung expressing GzmB (Fig. 5C). Increased numbers of $CD4^+$ and Ag-specific $CD8^+$ T cells were first detected in the lungs at day 7 and continued to increase at day 10 (Fig. 5A–B). Significantly more Ag-specific $CD8^+$ T cells were detected in the lungs of $Gzmb^{-/-}$ mice at day 10.

T_{reg} cells suppress $CD8^+$ T responses in a GzmB-dependent manner

Since $Gzmb^{-/-}$ mice exhibit a defect in regulating Ag-specific $CD8^+$ T cell responses, and since WT T_{reg} cells express GzmB *in vivo*, we next tested whether depletion of WT T_{reg} cells results in an expansion in Ag-specific $CD8^+$ T cells similar to that observed in $Gzmb^{-/-}$ mice. Pre-treating WT mice with anti-CD25 mAb at days -3 and -1 of SeV infection resulted in a significant decrease in the percentages of $FoxP3^+$ T_{reg} cell in the lungs (data not shown) and the draining lymph nodes (Fig. 6A) of infected animals. This reduction in the number of T_{reg} cells led to a significant increase in the percentages of Ag-specific $CD8^+$ T cells in the lungs of these mice (Fig. 6B). Importantly, the increase in the percentages of Ag-specific $CD8^+$ T cells was more pronounced in T_{reg} cell-depleted WT mice than T_{reg} cell-depleted $Gzmb^{-/-}$ mice, suggesting that the ability of T_{reg} cells to regulate Ag-specific $CD8^+$ T cell responses is mediated in part by GzmB.

The above studies demonstrate a role for GzmB in regulating Ag-specific $CD8^+$ T cell responses *in vivo*, and suggest that this effect may be mediated by T_{reg} cells. We next directly tested whether GzmB is required for T_{reg} cells to suppress $CD8^+$ T cell proliferation *in vitro*. WT T_{reg} cells were able to efficiently suppress $CD8^+$ T proliferation in a dosedependent manner, while $Gzmb^{-/-}$ T_{reg} cells displayed less suppression of $CD8^+$ T cell proliferation (Fig. 7). This supports our findings in the SeV model that T_{reg} cells regulate the immune responses to viral challenges in a GzmB-dependent manner.

Discussion

In this study we characterized the role of GzmB in immune regulation in a model of viral infection. Using the SeV model of acute respiratory bronchiolitis we demonstrated that *Gzmb*^{-/-} mice, despite having intact viral clearance, exhibited greater weight loss than WT mice. This correlated with an expansion of Ag-specific CD8⁺ T cells in the lungs and draining lymph nodes of these mice. We further characterized the expression of GzmB in WT mice in this model and demonstrated that, in addition to CD8⁺ T cells and NK cells, T_{reg} cells are efficient producers of GzmB, suggesting that GzmB expression in T_{reg} cells may be required to inhibit the expansion of Ag-specific CD8⁺ T cells. In support of this, depletion of T_{reg} cells in WT mice produced an expansion in Ag-specific CD8⁺ T cells similar to that observed in *Gzmb*^{-/-} mice. Furthermore, *Gzmb*^{-/-} T_{reg} cells were deficient in their ability to suppress CD8⁺ T cell proliferation *in vitro*.

Infection of *Prf1*^{-/-} mice with LCMV, MCMV, and Respiratory syncytial virus (RSV) is known to result in severe inflammatory responses with features of HLH along with failure to clear viral challenges^{9;13;44;45}. Depletion of CD8⁺ T cells, IFN- γ ¹³, or TNF- α ⁹ ameliorates the increased mortality in these mice, arguing that CD8⁺ T cell-driven immune pathology is responsible for the observed morbidity and mortality. One possible explanation for these observations is that persistence of viral Ags, due to failure in viral clearance, results in prolonged and excessive CD8⁺ T cell activation, cytokine production, and immune pathology. However, in our model *Gzmb*^{-/-} mice infected with SeV displayed viral titers comparable to WT mice indicating that GzmB is not essential for SeV clearance. While this is not surprising, due to redundancy in the antiviral roles of Gzms^{8;9;46}, the expansion of Ag-specific CD8⁺ T cells and the corresponding enhanced weight loss in *Gzmb*^{-/-} mice demonstrate a regulatory role for GzmB independent of its role in viral clearance.

These studies suggest that GzmB-expressing T_{reg} cells contribute to the control of Ag-specific CD8⁺ T cells. In our model, we observed a significant increase in the number of T_{reg} cells in the lungs of SeV infected mice. The majority of these cells expressed GzmB at day 7, indicating that viral infection is a potent inducer of GzmB expression in T_{reg} cells. In addition, T_{reg} cell depletion of WT mice with monoclonal antibodies to CD25 resulted in an increase in the percentages of Ag-specific CD8⁺ T cells similar to that seen in untreated *Gzmb*^{-/-} mice. Finally, *Gzmb*^{-/-} T_{reg} cells demonstrated a reduced capacity to suppress CD8⁺ T cell proliferation *in vitro*. Although a role for GzmB expressed by cells other than T_{reg} cells, such as Ag-specific CD8⁺ T cells and NK cells, cannot be ruled out, our data suggests a specific immune-regulatory role for GzmB in the T_{reg} cell compartment in response to viral infection. Supporting these observations is the enhanced survival of *Gzmb*^{-/-} mice to syngeneic tumor challenges due to inability of T_{reg} cells in these mice to suppress effective CD8⁺ T and NK cell anti-tumor responses¹⁵. Similarly, FoxP3⁺ T_{reg} cells were shown to induce dendritic cell death in a Prf-dependent manner in tumor draining lymph nodes, thereby limiting the onset of CD8⁺ T cell anti-tumor responses⁴⁷. Additionally, different groups have demonstrated that T_{reg} cells are recruited to sites of infection, and that immune responses specific to viruses are enhanced when CD4⁺CD25⁺ T_{reg} cells are depleted *in vivo*^{4;48-50}.

The increase in the number of Ag-specific CD8⁺ T cells in the lungs of *Gzmb*^{-/-} mice indicates that GzmB in T_{reg} cells regulates either the initiation of Ag-specific CD8⁺ T cell responses or the down modulation of terminal effector cells, or a combination of both. In addition, preliminary data from our lab show a trend toward increased antigen specific CD8 cells and total CD8 cells in the lungs of *Gzmb*^{-/-} 55 days after infection, suggesting that control of the primary CD8⁺ T response may affect the magnitude of a memory response(data not shown). So far, *in vivo* studies have been inconclusive about the exact

nature of the targets of GzmB- T_{reg} cell-mediated immune suppression. Tumor infiltrating CD8⁺ T cells and NK cells in one model¹⁵, dendritic cells in another model⁴⁷, and CD4⁺ T cells (but not CD8⁺ T cells) in yet another model²⁹ have all been implicated. In our SeV model, T_{reg} cells did not exhibit significant upregulation of GzmB until day 7. Additionally, there were no significant differences in the numbers or percentages of dendritic cells or B cells in either the lungs or the draining lymph nodes of *Gzmb*^{-/-} mice. While this does not preclude a regulatory role for GzmB in the priming of the immune response by means other than inducing apoptosis of APCs or CD4 cells, we propose that GzmB has a direct down-modulating effect on Ag-specific effector CD8⁺ T cells. Whether this effect occurs in the lungs and/or the draining lymph remains to be seen. In support of this, the enhanced survival of *Gzmb*^{-/-} mice in the tumor challenge model¹⁵ was attributed to the direct decrease in killing of CD8⁺ T cells and NK cells by tumor-infiltrating T_{reg} cells deficient in GzmB. A direct down-modulating effect on Ag-specific CD8⁺ T cells as they are expanding would limit immune regulation to cells that are responsible for the observed immune-pathology after allowing for initiation of effective anti-viral immune responses.

One interesting finding in these studies was that *Gzmb*^{-/-} mice exhibited a significant increase in the percentages of CD25⁺Ag-specific CD8⁺ T cells, which could result in enhanced responsiveness to IL-2 and increased proliferation of these cells. This raises the possibility that GzmB in T_{reg} cells is responsible for down regulation of CD25 expression in target CD8⁺ T cells, thereby allowing for selective down modulation of their responsiveness to IL-2, which in turn is critical for their ability to produce IFN- γ and for their cytotoxic function⁵¹⁻⁵². Indeed, WT CD4⁺CD25⁺ T_{reg} cells were shown to suppress CD25 expression and IFN- γ production in responding CD8⁺ T cells in co-culture studies⁵³. How T_{reg} cells inhibit CD25 expression is unclear. Inhibition of APC function or induction of apoptosis in APCs could limit the extent of CD8⁺ T cell activation and CD25 expression. Alternatively, GzmB delivered directly to CD8⁺ T cells could affect expression of CD25 independently from its proapoptotic function. This may explain the observation that T_{reg} cells are able to inhibit lymphocyte responses in a Prf independent manner²⁴. Further investigations are required to address these possibilities.

In summary, our findings identify a unique role for GzmB in regulating Ag-specific CD8⁺ T responses in the context of viral infection. They also suggest that this role is mediated, in part, by the T_{reg} cell compartment.

Acknowledgments

We thank Drs. Michael Holtzman and Eugene Agapov for the kind gift of the SeV qPCR primers and probe.

This work was supported by the Children's Hospital of Wisconsin Foundation and the NIH (N01A150032, K08AI072023) (to J.W.V.) and (R01HL087778) (to M.H.G.)

Reference List

1. Lieberman J. The ABCs of granule-mediated cytotoxicity: new weapons in the arsenal. *Nat Rev Immunol.* 2003; 3:361-370. [PubMed: 12766758]
2. Trapani JA, Smyth MJ. Functional significance of the perforin/granzyme cell death pathway. *Nat Rev Immunol.* 2002; 2:735-747. [PubMed: 12360212]
3. Kagi D, Ledermann B, Burki K, Seiler P, Odermatt B, Olsen KJ, Podack ER, Zinkernagel RM, Hengartner H. Cytotoxicity mediated by T cells and natural killer cells is greatly impaired in perforin-deficient mice. *Nature.* 1994; 369:31-37. [PubMed: 8164737]
4. Zelinsky G, Balkow S, Schimmer S, Schepers K, Simon MM, Dittmer U. Independent roles of perforin, granzymes, and Fas in the control of Friend retrovirus infection. *Virology.* 2004; 330:365-374. [PubMed: 15567431]

5. Simon MM, Hausmann M, Tran T, Ebnet K, Tschopp J, ThaHla R, Mullbacher A. In vitro- and ex vivo-derived cytolytic leukocytes from granzyme A x B double knockout mice are defective in granule-mediated apoptosis but not lysis of target cells. *J Exp Med*. 1997; 186:1781–1786. [PubMed: 9362539]
6. Ebnet K, Hausmann M, Lehmann-Grube F, Mullbacher A, Kopf M, Lamers M, Simon MM. Granzyme A-deficient mice retain potent cell-mediated cytotoxicity. *EMBO J*. 1995; 14:4230–4239. [PubMed: 7556064]
7. Zajac AJ, Dye JM, Quinn DG. Control of lymphocytic choriomeningitis virus infection in granzyme B deficient mice. *Virology*. 2003; 305:1–9. [PubMed: 12504535]
8. Loh J, Thomas DA, Revell PA, Ley TJ, Virgin HW. Granzymes and caspase 3 play important roles in control of gammaherpesvirus latency. *J Virol*. 2004; 78:12519–12528. [PubMed: 15507639]
9. van Dommelen SL, Sumaria N, Schreiber RD, Scalzo AA, Smyth MJ, Degli-Esposti MA. Perforin and granzymes have distinct roles in defensive immunity and immunopathology. *Immunity*. 2006; 25:835–848. [PubMed: 17088087]
10. Filipovich AH. Hemophagocytic lymphohistiocytosis and related disorders. *Curr Opin Allergy Clin Immunol*. 2006; 6:410–415. [PubMed: 17088644]
11. Stepp SE, Dufourcq-Lagelouse R, Le Deist F, Bhawan S, Certain S, Mathew PA, Henter JI, Bennett M, Fischer A, Saint Basile G, Kumar V. Perforin gene defects in familial hemophagocytic lymphohistiocytosis. *Science*. 1999; 286:1957–1959. [PubMed: 10583959]
12. Verbsky JW, Grossman WJ. Hemophagocytic lymphohistiocytosis: diagnosis, pathophysiology, treatment, and future perspectives. *Ann Med*. 2006; 38:20–31. [PubMed: 16448985]
13. Badovinac VP, Hamilton SE, Harty JT. Viral infection results in massive CD8+ T cell expansion and mortality in vaccinated perforin-deficient mice. *Immunity*. 2003; 18:463–474. [PubMed: 12705850]
14. Belkaid Y, Piccirillo CA, Mendez S, Shevach EM, Sacks DL. CD4+CD25+ regulatory T cells control *Leishmania* major persistence and immunity. *Nature*. 2002; 420:502–507. [PubMed: 12466842]
15. Cao X, Cai SF, Fehniger TA, Song J, Collins LI, Piwnica-Worms DR, Ley TJ. Granzyme B and perforin are important for regulatory T cell-mediated suppression of tumor clearance. *Immunity*. 2007; 27:635–646. [PubMed: 17919943]
16. Haribhai D, Lin W, Relland LM, Truong N, Williams CB, Chatila TA. Regulatory T cells dynamically control the primary immune response to foreign antigen. *J Immunol*. 2007; 178:2961–2972. [PubMed: 17312141]
17. Sakaguchi S. Naturally arising CD4+ regulatory t cells for immunologic self-tolerance and negative control of immune responses. *Annu Rev Immunol*. 2004; 22:531–562. [PubMed: 15032588]
18. Fontenot JD, Gavin MA, Rudensky AY. Foxp3 programs the development and function of CD4+CD25+ regulatory T cells. *Nat Immunol*. 2003; 4:330–336. [PubMed: 12612578]
19. Hori S, Nomura T, Sakaguchi S. Control of regulatory T cell development by the transcription factor Foxp3. *Science*. 2003; 299:1057–1061. [PubMed: 12522256]
20. Thornton AM, Shevach EM. CD4+CD25+ immunoregulatory T cells suppress polyclonal T cell activation in vitro by inhibiting interleukin 2 production. *J Exp Med*. 1998; 188:287–296. [PubMed: 9670041]
21. Grossman WJ, Verbsky JW, Barchet W, Colonna M, Atkinson JP, Ley TJ. Human T regulatory cells can use the perforin pathway to cause autologous target cell death. *Immunity*. 2004; 21:589–601. [PubMed: 15485635]
22. Shevach EM. Mechanisms of foxp3+ T regulatory cell-mediated suppression. *Immunity*. 2009; 30:636–645. [PubMed: 19464986]
23. von Boehmer H. Mechanisms of suppression by suppressor T cells. *Nat Immunol*. 2005; 6:338–344. [PubMed: 15785759]
24. Gondek DC, Lu LF, Quezada SA, Sakaguchi S, Noelle RJ. Cutting edge: contact-mediated suppression by CD4+CD25+ regulatory cells involves a granzyme B-dependent, perforin-independent mechanism. *J Immunol*. 2005; 174:1783–1786. [PubMed: 15699103]

25. Zhao DM, Thornton AM, DiPaolo RJ, Shevach EM. Activated CD4+CD25+ T cells selectively kill B lymphocytes. *Blood*. 2006; 107:3925–3932. [PubMed: 16418326]
26. Phillips T, Opferman JT, Shah R, Liu N, Froelich CJ, Ashton-Rickardt PG. A role for the granzyme B inhibitor serine protease inhibitor 6 in CD8+ memory cell homeostasis. *J Immunol*. 2004; 173:3801–3809. [PubMed: 15356127]
27. Sun J, Ooms L, Bird CH, Sutton VR, Trapani JA, Bird PI. A new family of 10 murine ovalbumin serpins includes two homologs of proteinase inhibitor 8 and two homologs of the granzyme B inhibitor (proteinase inhibitor 9). *J Biol Chem*. 1997; 272:15434–15441. [PubMed: 9182575]
28. Zhang M, Park SM, Wang Y, Shah R, Liu N, Murmann AE, Wang CR, Peter ME, Ashton-Rickardt PG. Serine protease inhibitor 6 protects cytotoxic T cells from self-inflicted injury by ensuring the integrity of cytotoxic granules. *Immunity*. 2006; 24:451–461. [PubMed: 16618603]
29. Gondek DC, Devries V, Nowak EC, Lu LF, Bennett KA, Scott ZA, Noelle RJ. Transplantation survival is maintained by granzyme B+ regulatory cells and adaptive regulatory T cells. *J Immunol*. 2008; 181:4752–4760. [PubMed: 18802078]
30. Faisca P, Desmecht D. Sendai virus, the mouse parainfluenza type 1: a longstanding pathogen that remains up-to-date. *Res Vet Sci*. 2007; 82:115–125. [PubMed: 16759680]
31. Tashiro M, Yokogoshi Y, Tobita K, Seto JT, Rott R, Kido H. Tryptase Clara, an activating protease for Sendai virus in rat lungs, is involved in pneumopathogenicity. *J Virol*. 1992; 66:7211–7216. [PubMed: 1331518]
32. Walter MJ, Morton JD, Kajiwaru N, Agapov E, Holtzman MJ. Viral induction of a chronic asthma phenotype and genetic segregation from the acute response. *J Clin Invest*. 2002; 110:165–175. [PubMed: 12122108]
33. Iwai H, Machii K, Otsuka Y, Ueda K. T cells subsets responsible for clearance of Sendai virus from infected mouse lungs. *Microbiol Immunol*. 1988; 32:305–315. [PubMed: 2839753]
34. Iwai H, Yamamoto S, Otsuka Y, Ueda K. Cooperation between humoral factor(s) and Lyt-2+ T cells in effective clearance of Sendai virus from infected mouse lungs. *Microbiol Immunol*. 1989; 33:915–927. [PubMed: 2574407]
35. Cole GA, Hogg TL, Woodland DL. The MHC class I-restricted T cell response to Sendai virus infection in C57BL/6 mice: a single immunodominant epitope elicits an extremely diverse repertoire of T cells. *Int Immunol*. 1994; 6:1767–1775. [PubMed: 7865469]
36. Cole GA, Hogg TL, Coppola MA, Woodland DL. Efficient priming of CD8+ memory T cells specific for a subdominant epitope following Sendai virus infection. *J Immunol*. 1997; 158:4301–4309. [PubMed: 9126992]
37. Hou S, Doherty PC, Zijlstra M, Jaenisch R, Katz JM. Delayed clearance of Sendai virus in mice lacking class I MHC-restricted CD8+ T cells. *J Immunol*. 1992; 149:1319–1325. [PubMed: 1354233]
38. Kast WM, Roux L, Curren J, Blom HJ, Voordouw AC, Meloen RH, Kolakofsky D, Melief CJ. Protection against lethal Sendai virus infection by in vivo priming of virus-specific cytotoxic T lymphocytes with a free synthetic peptide. *Proc Natl Acad Sci U S A*. 1991; 88:2283–2287. [PubMed: 1848698]
39. Revell PA, Grossman WJ, Thomas DA, Cao X, Behl R, Ratner JA, Lu ZH, Ley TJ. Granzyme B and the downstream granzymes C and/or F are important for cytotoxic lymphocyte functions. *J Immunol*. 2005; 174:2124–2131. [PubMed: 15699143]
40. Kim EY, Battaile JT, Patel AC, You Y, Agapov E, Grayson MH, Benoit LA, Byers DE, Alevy Y, Tucker J, Swanson S, Tidwell R, Tyner JW, Morton JD, Castro M, Polineni D, Patterson GA, Schwendener RA, Allard JD, Peltz G, Holtzman MJ. Persistent activation of an innate immune response translates respiratory viral infection into chronic lung disease. *Nat Med*. 2008; 14:633–640. [PubMed: 18488036]
41. Kohm AP, McMahon JS, Podojil JR, Begolka WS, DeGutes M, Kasprovicz DJ, Ziegler SF, Miller SD. Cutting Edge: Anti-CD25 monoclonal antibody injection results in the functional inactivation, not depletion, of CD4+CD25+ T regulatory cells. *J Immunol*. 2006; 176:3301–3305. [PubMed: 16517695]

42. Onizuka S, Tawara I, Shimizu J, Sakaguchi S, Fujita T, Nakayama E. Tumor rejection by in vivo administration of anti-CD25 (interleukin-2 receptor alpha) monoclonal antibody. *Cancer Res.* 1999; 59:3128–3133. [PubMed: 10397255]
43. Usherwood EJ, Hogan RJ, Crowther G, Surman SL, Hogg TL, Altman JD, Woodland DL. Functionally heterogeneous CD8(+) T-cell memory is induced by Sendai virus infection of mice. *J Virol.* 1999; 73:7278–7286. [PubMed: 10438816]
44. Aung S, Rutigliano JA, Graham BS. Alternative mechanisms of respiratory syncytial virus clearance in perforin knockout mice lead to enhanced disease. *J Virol.* 2001; 75:9918–9924. [PubMed: 11559824]
45. Matloubian M, Suresh M, Glass A, Galvan M, Chow K, Whitmire JK, Walsh CM, Clark WR, Ahmed R. A role for perforin in downregulating T-cell responses during chronic viral infection. *J Virol.* 1999; 73:2527–2536. [PubMed: 9971838]
46. Bem RA, van Woensel JB, Lutter R, Domachowske JB, Medema JP, Rosenberg HF, Bos AP. Granzyme A- and B-cluster deficiency delays acute lung injury in pneumovirus-infected mice. *J Immunol.* 184:931–938. [PubMed: 20018616]
47. Boissonnas A, Scholer-Dahirel A, Simon-Blancal V, Pace L, Valet F, Kissenpfennig A, Sparwasser T, Malissen B, Fetler L, Amigorena S. Foxp3+ T cells induce perforin-dependent dendritic cell death in tumor-draining lymph nodes. *Immunity.* 32:266–278. [PubMed: 20137985]
48. Dittmer U, He H, Messer RJ, Schimmer S, Olbrich AR, Ohlen C, Greenberg PD, Stromnes IM, Iwashiro M, Sakaguchi S, Evans LH, Peterson KE, Yang G, Hasenkrug KJ. Functional impairment of CD8(+) T cells by regulatory T cells during persistent retroviral infection. *Immunity.* 2004; 20:293–303. [PubMed: 15030773]
49. Rouse BT, Sarangi PP, Suvas S. Regulatory T cells in virus infections. *Immunol Rev.* 2006; 212:272–286. [PubMed: 16903920]
50. Suvas S, Kumaraguru U, Pack CD, Lee S, Rouse BT. CD4+CD25+ T cells regulate virus-specific primary and memory CD8+ T cell responses. *J Exp Med.* 2003; 198:889–901. [PubMed: 12975455]
51. Mosmann TR, Sad S, Krishnan L, Wegmann TG, Guilbert LJ, Belosevic M. Differentiation of subsets of CD4+ and CD8+ T cells. *Ciba Found Symp.* 1995; 195:42–50. [PubMed: 8724829]
52. Sad S, Krishnan L. Cytokine deprivation of naive CD8+ T cells promotes minimal cell cycling but maximal cytokine synthesis and autonomous proliferation subsequently: a mechanism of self-regulation. *J Immunol.* 1999; 163:2443–2451. [PubMed: 10452979]
53. Piccirillo CA, Shevach EM. Cutting edge: control of CD8+ T cell activation by CD4+CD25+ immunoregulatory cells. *J Immunol.* 2001; 167:1137–1140. [PubMed: 11466326]

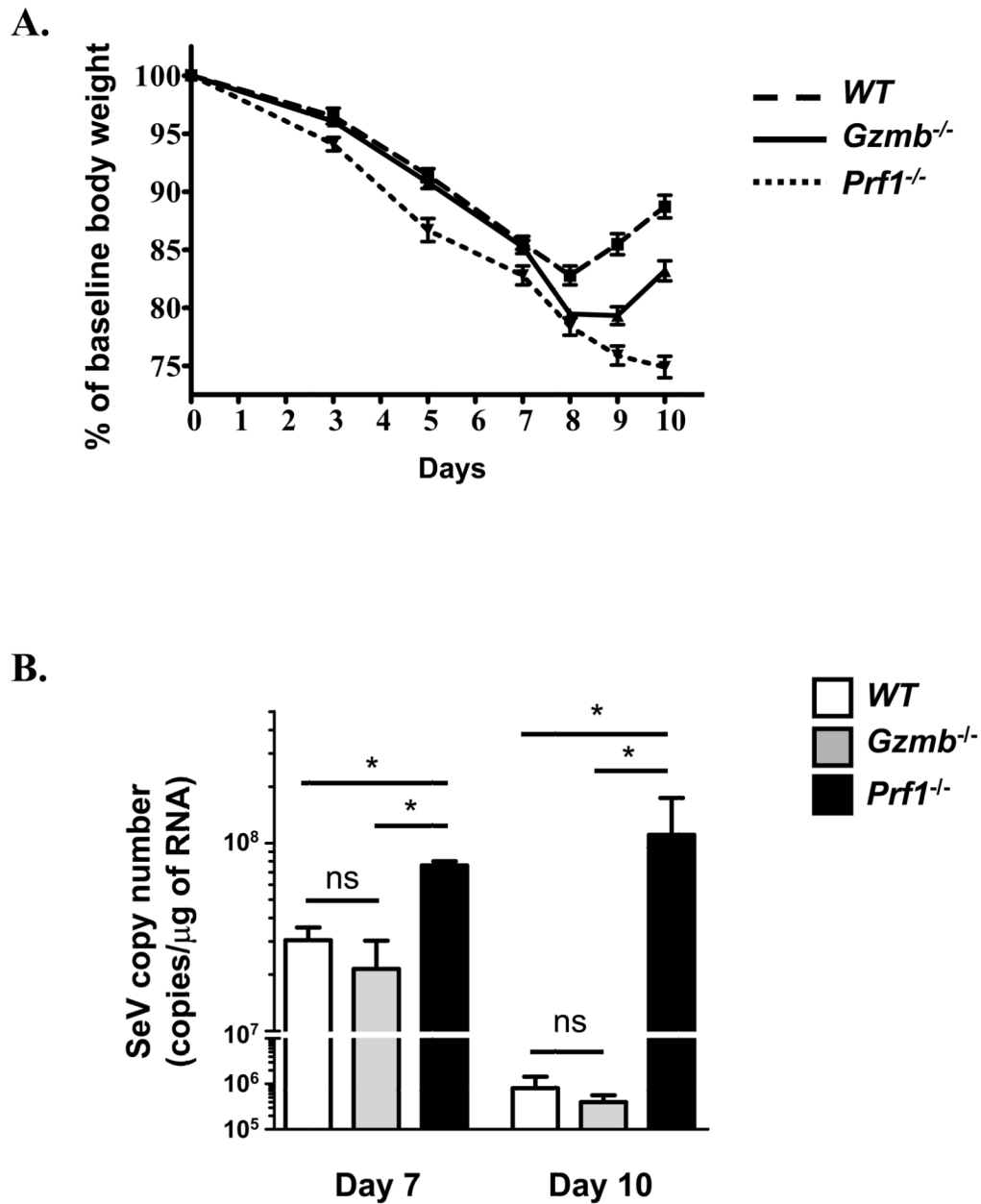


Figure 1. Response to SeV infection

A. Weight loss of WT, *Gzmb*^{-/-}, and *Prf1*^{-/-} mice infected with 6×10^4 PFU SeV depicted as percent weight loss from baseline (n=50 for WT, 52 for *Gzmb*^{-/-} mice, and 28 for *Prf1*^{-/-} mice). Significant differences in weight loss were detected at day 8 (WT vs. *Prf1*^{-/-}, $p < 0.01$; WT vs *Gzmb*^{-/-}, $p < 0.01$), day 9 (WT vs. *Prf1*^{-/-}, $p < 0.001$; WT vs *Gzmb*^{-/-}, $p < 0.001$; *Prf1*^{-/-} vs. *Gzmb*^{-/-}, $p < 0.05$) and day 10 (WT vs. *Prf1*^{-/-}, $p < 0.001$; WT vs *Gzmb*^{-/-}, $p < 0.001$; *Prf1*^{-/-} vs. *Gzmb*^{-/-}, $p < 0.001$). Significance was determined by Two-way repeated measures ANOVA. **B.** Viral RNA copy number in the lungs was determined at days 7 and 10 by real-time RT-PCR for SeV nucleocapsid protein. (n=3–6 mice in each group from 2 separate experiments, *, $p < 0.05$).

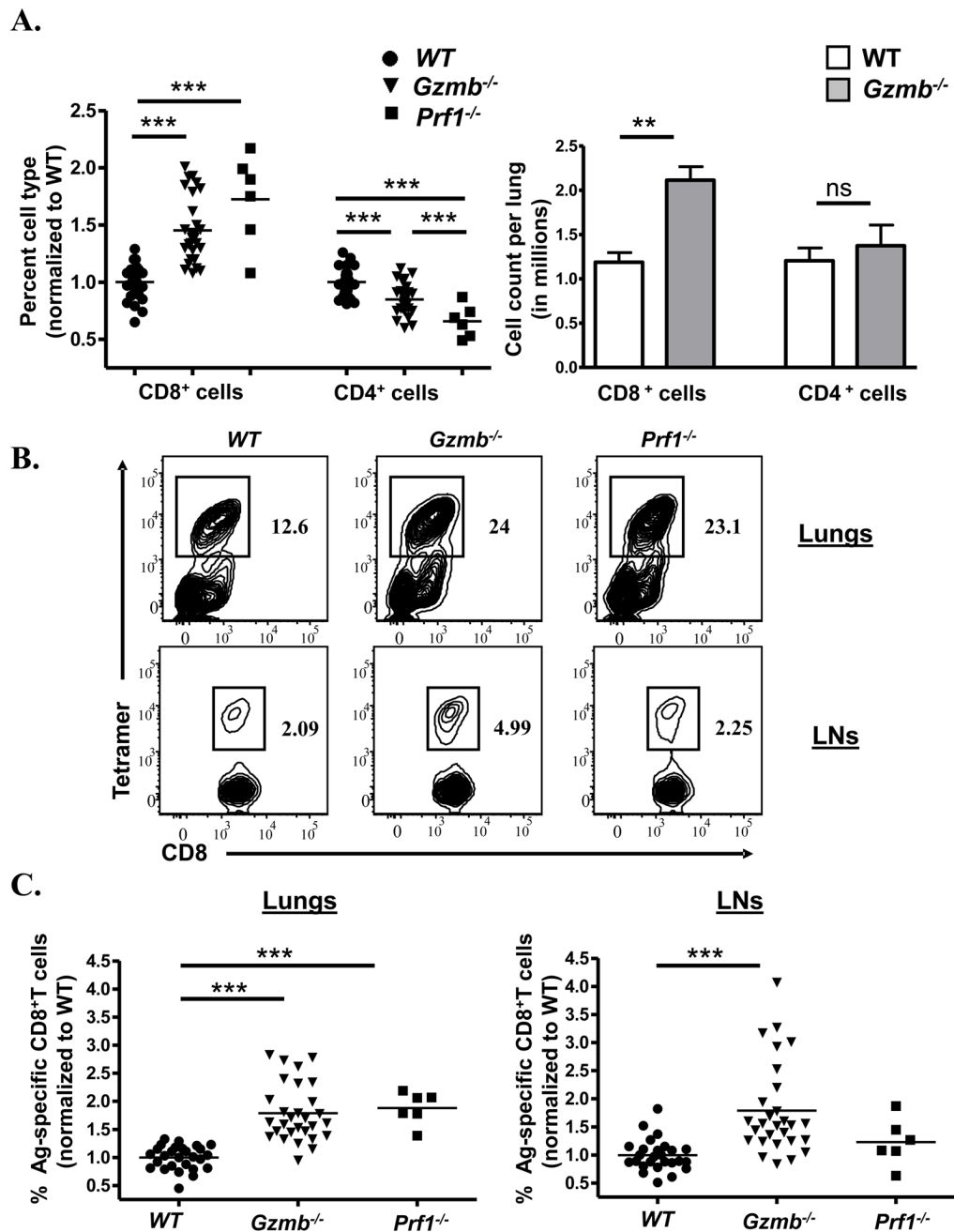


Figure 2. Expansion of CD8⁺ T cell compartment in the lungs of *Gzmb*^{-/-} mice and *Prf1*^{-/-} mice in response to SeV infection

WT, *Gzmb*^{-/-}, and *Prf1*^{-/-} mice were infected with 6×10^4 PFU SeV and lungs analyzed by flow cytometry. **A.** Left: Percent CD4⁺ and CD8⁺ T cells from live cell gate in the lungs following SeV infection. Results from each experiment were normalized to WT, and data presented as fold increase over WT samples. Right: Absolute cell count in the lungs following SeV infection. **B.** Representative FACS plots demonstrating Ag-specific CD8⁺ T cells in the lungs and draining lymph nodes of infected animals. The plots from the lymph nodes were first gated on CD8⁺ T cells. **C.** Percent of CD8⁺ T cells that are tetramer positive was determined in the lungs and draining lymph node following SeV infection, then

normalized to WT mice (n=27 for WT mice, 29 for *Gzmb*^{-/-} mice, and 6 for *Prfl*^{-/-} mice, **, $p < 0.01$; and ***, $p < 0.001$).

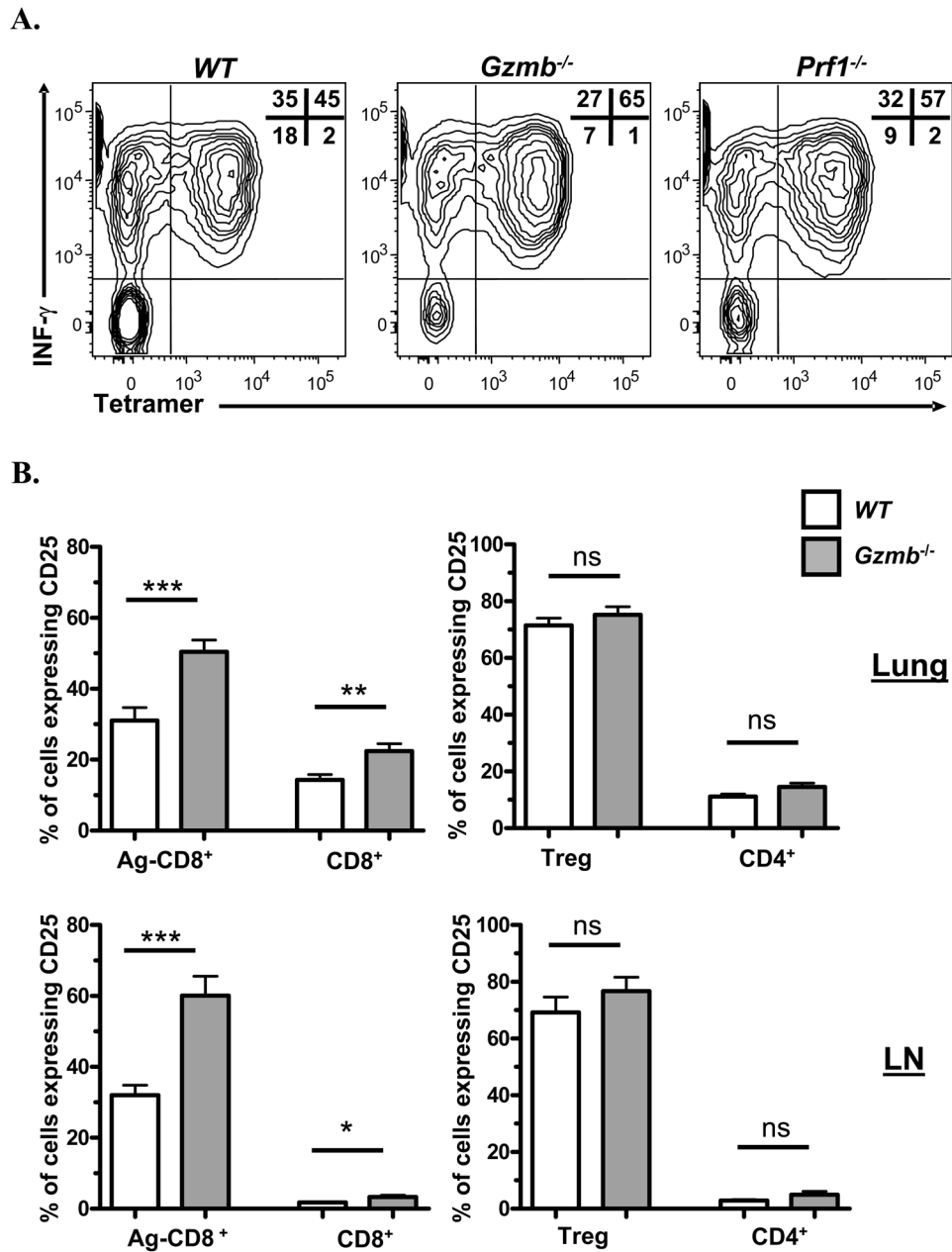


Figure 3. Expression of IFN- γ and CD25 in Ag-specific CD8⁺ T cells in response to SeV infection
A. WT, *Gzmb*^{-/-}, and *Prf1*^{-/-} mice were infected with 6×10^4 PFU SeV, lymphocytes were isolated from the lungs, stimulated with PMA/ionomycin, and IFN- γ was detected by intracellular staining. Representative FACS plots showing IFN- γ expression in Ag specific and non-Ag specific CD8⁺ T cells. FACS plots were gated on CD8 cells. **B.** The percent of conventional CD4⁺ T cells, T_{reg} cells, and Ag-specific and non Ag-specific CD8⁺ T cells expressing CD25 was determined by flow cytometry (*, $p < 0.05$; **, $p < 0.01$; and ***, $p < 0.001$).

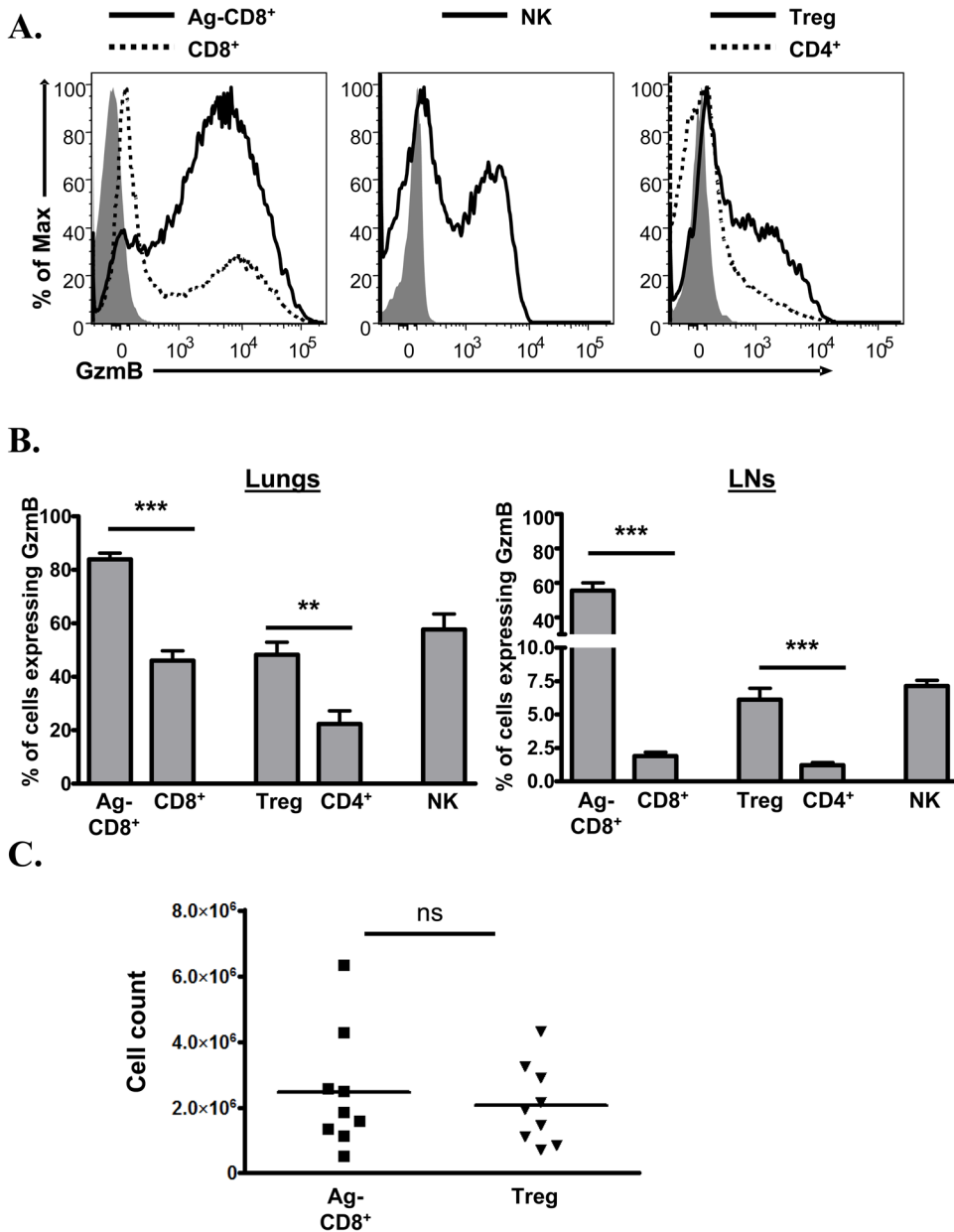


Figure 4. GzmB expression in immune effector cells in response to SeV infection
 WT Foxp3^{EGFP} locus-tagged mice were infected with 6×10⁴ PFU SeV and analyzed for GzmB expression 10 days later. **A.** Representative histograms showing GzmB expression in different cell populations in the lungs of an infected animal. Shaded histogram represents background staining using *Gzmb*^{-/-} mouse. **B.** Expression of GzmB was determined by flow cytometry and depicted as the percent of each cell population expressing GzmB in the lungs and draining lymph nodes. **C.** Absolute number of GzmB⁺ T_{regs} cells and GzmB⁺ Ag-specific CD8⁺ T cells was determined from the draining lymph nodes (**, *p*<0.01; and ***, *p*<0.001).

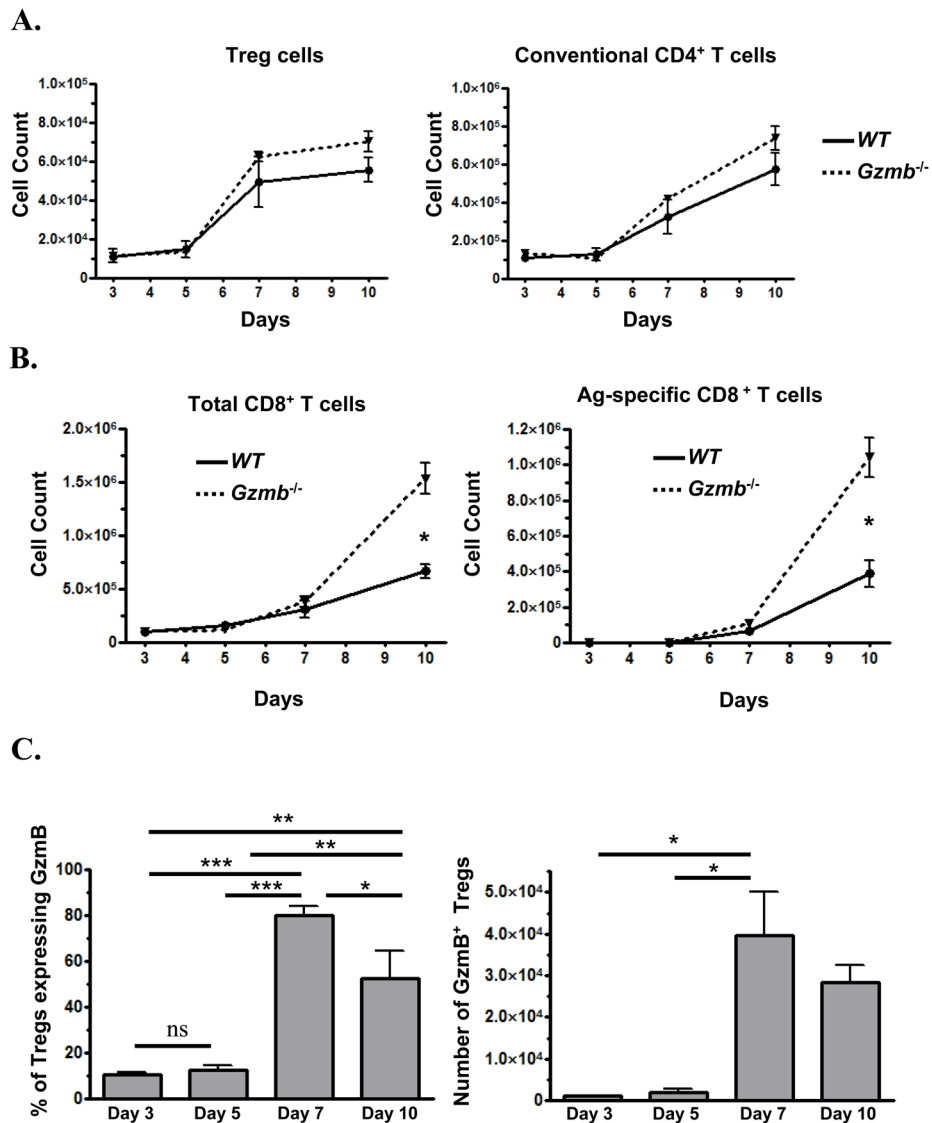


Figure 5. GzmB-expressing T_{reg} cells are recruited to the lungs in response to SeV infection
 WT Foxp3^{EGFP} mice were infected with 6×10^4 PFU SeV and analyzed for EGFP and GzmB expression at days 3, 5, 7, and 10. **A.** Quantification of T_{regs} cell and conventional CD4⁺ T cell numbers in the lungs. **B.** Quantification of total CD8⁺ T cell and Ag-specific CD8⁺ T cell numbers in the lungs. **C.** Percent (Left), and absolute count of GzmB⁺ T_{regs} cells (Right) in the lungs of infected animals (*, $p < 0.05$; **, $p < 0.01$; and ***, $p < 0.001$).

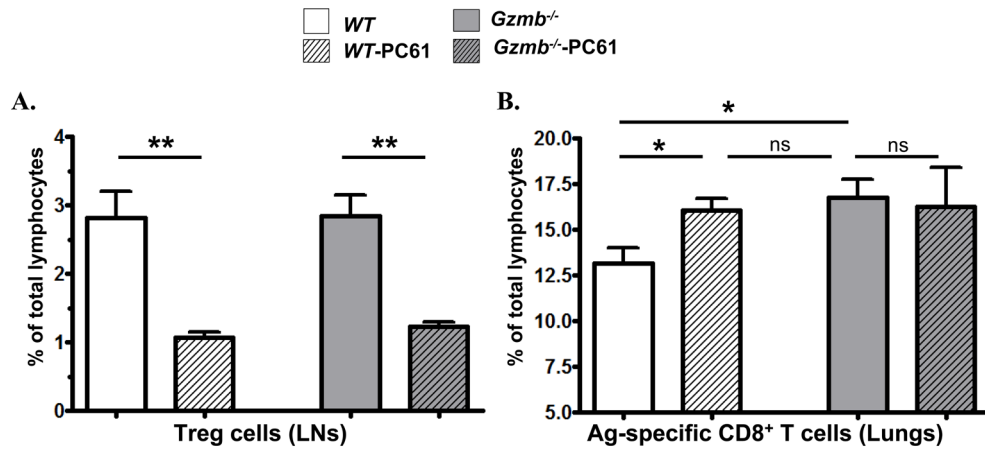


Figure 6. Depletion of T_{reg} cells results in expansion of Ag-specific CD8⁺ T cells in the lungs of WT mice in response to SeV infection

WT mice and *Gzmb*^{-/-} mice were pre-treated with anti CD25 mAb (PC61) or isotype at days -3 and -1, followed by infection with 6×10^4 PFU SeV. Lungs were analyzed for EGFP⁺CD4⁺ T_{reg} cells and Ag-specific CD8⁺ T cells 10 days later. A. Percent of T_{reg} cells in the draining lymph nodes of infected animals. B. Percent of Ag-specific CD8 cells in the lungs of infected animals (n=6 mice per group) (*, $p < 0.05$; and **, $p < 0.01$).

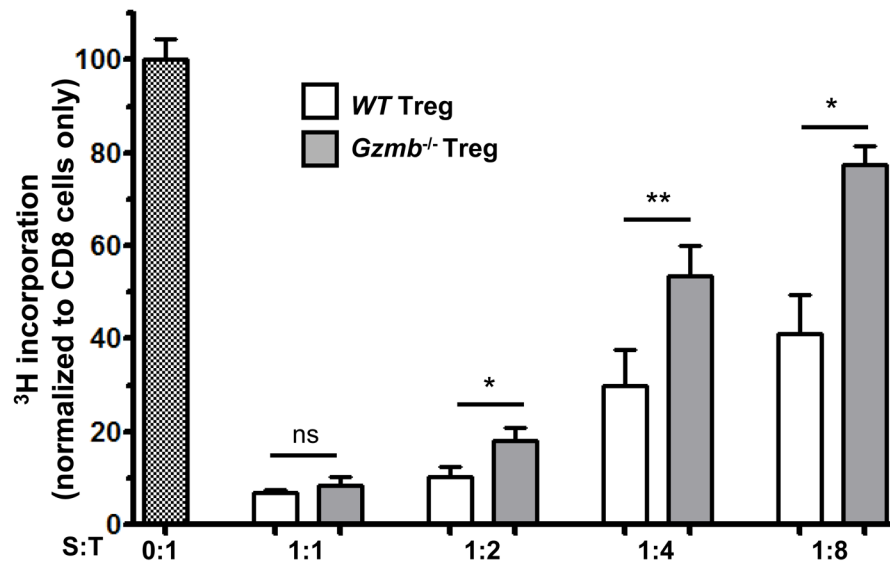


Figure 7. T_{regs} cells suppress CD8⁺ T cell proliferation in a GzmB-dependent manner
 WT CD8⁺ T cells were cultured with WT or *Gzmb*^{-/-} T_{reg} cells in the indicated suppressor:target ratios (S:T) and stimulated with soluble anti-CD3 mAb. Proliferation of CD8⁺ T cells was assessed by [³H]thymidine incorporation at day 4. Data are the average of 9 replicates from 3 independent experiments normalized to CD8⁺ T cells proliferation without added T_{reg} cells (*, $p < 0.05$; and **, $p < 0.01$).